Check for updates

Geophysical Research Letters

RESEARCH LETTER
10.1029/2022GL101605

Methanol Concentrations and Biological Methanol Consumption in the Northwest Pacific Ocean

Zhen Zhou[1,2,3], Guang-Chao Zhuang[1,2,3], Shi-Hai Mao[1,2,3], Jiarui Liu[4], Xiao-Jun Li[1,2,3], Qiao Liu[1,2,3], Guo-Dong Song[1,2,3], Hong-Hai Zhang[1,2,3], Zhaohui Chen[5], Andrew Montgomery[6], Samantha Joye[7], and Gui-Peng Yang[1,2,3]

[1]Key Laboratory of Marine Chemistry Theory and Technology, Frontiers Science Center for Deep Ocean Multispheres and Earth System, Ministry of Education, Ocean University of China, Qingdao, China, [2]Laboratory of Marine Ecology and Environmental Science, Qingdao National Laboratory for Marine Science and Technology, Qingdao, China, [3]College of Chemistry and Chemical Engineering, Ocean University of China, Qingdao, China, [4]Department of Earth, Planetary and Space Sciences, University of California, Los Angeles, Los Angeles, CA, USA, [5]Key Laboratory of Physical Oceanography, Frontiers Science Center for Deep Ocean Multispheres and Earth System, Ocean University of China, Qingdao, China, [6]Department of Chemistry and Biochemistry, Montana State University, Bozeman, MT, USA, [7]Department of Marine Sciences, University of Georgia, Athens, GA, USA

Key Points:

- Methanol was detected in relatively low concentrations due to rapid biological consumption in the Kuroshio-Oyashio extension region
- Much higher oxidation rates than assimilation rates suggested methanol was predominantly used as an energy source
- Atmospheric deposition is a source of methanol in the mixed layer and accounted for 22.7% of microbial methanol consumption

Supporting Information:

Supporting Information may be found in the online version of this article.

Correspondence to:

G.-C. Zhuang,
zgc@ouc.edu.cn

Citation:

Zhou, Z., Zhuang, G.-C., Mao, S.-H., Liu, J., Li, X.-J., Liu, Q., et al. (2023). Methanol concentrations and biological methanol consumption in the northwest Pacific Ocean. *Geophysical Research Letters*, *50*, e2022GL101605. https://doi.org/10.1029/2022GL101605

Received 13 OCT 2022
Accepted 31 MAR 2023

Author Contributions:

Conceptualization: Zhen Zhou, Guang-Chao Zhuang, Samantha Joye
Data curation: Zhen Zhou, Qiao Liu
Formal analysis: Hong-Hai Zhang
Funding acquisition: Guang-Chao Zhuang
Investigation: Zhen Zhou, Shi-Hai Mao, Xiao-Jun Li, Qiao Liu, Guo-Dong Song, Zhaohui Chen
Methodology: Zhen Zhou, Guang-Chao Zhuang, Shi-Hai Mao, Xiao-Jun Li, Qiao Liu, Guo-Dong Song, Hong-Hai Zhang, Zhaohui Chen

© 2023 The Authors.
This is an open access article under the terms of the Creative Commons Attribution-NonCommercial License, which permits use, distribution and reproduction in any medium, provided the original work is properly cited and is not used for commercial purposes.

Abstract Methanol metabolism can play an important role in marine carbon cycling. We made contemporaneous measurements of methanol concentration and consumption rates in the northwest Pacific Ocean to constrain the pathways and dynamics of methanol cycling. Methanol was detected in relatively low concentrations (<12–391 nM), likely due to rapid biological turnover. Rates of methanol oxidation to CO_2 (0.9–130.5 nmol L^{-1} day^{-1}) were much higher than those of assimilation into biomass (0.09–6.8 nmol L^{-1} day^{-1}), suggesting that >89.7% of methanol was utilized as an energy source. Surface water acted as a net methanol sink at most sites, with an average flux of 9 μmol L^{-1} day^{-1}. Atmospheric deposition accounted for 22.7% of microbial methanol consumption in the mixed layer, illustrating that the atmosphere is less important than internal processes for driving methanol cycling in these pelagic waters.

Plain Language Summary Methanol is one of the most abundant oxygenated volatile organic compounds in the atmosphere and microbial methanol metabolism is an important part of the marine carbon cycle. However, only a limited number of studies describe methanol cycling in marine waters, and the sources and sinks of methanol remain largely unconstrained in the Pacific Ocean. We investigated the distribution and microbial consumption of methanol in the Kuroshio-Oyashio extension region of northwest Pacific Ocean. Methanol was used primarily as an energy source and the rapid biological turnover of methanol contributed to relatively low-standing stocks of methanol. Air-sea flux estimates suggested that the atmosphere was a net source of methanol to the study area. Compared to in situ production and consumption rates, air-sea exchange represented a less important process for methanol cycling in the mixed layer. Our results add to the global database of methanol concentrations and help to constrain the biological sources and sinks of methanol in the surface ocean.

1. Introduction

Methanol is one of the most abundant oxygenated volatile organic compounds in the atmosphere and plays an important role in atmospheric chemistry and ocean ecology (Heikes et al., 2002; Singh et al., 2001; Zhuang et al., 2018). Due to the variability of methanol concentrations and sea-air exchange fluxes between locations, uncertainty remains as to whether the ocean is a source or sink of atmospheric methanol. For example, Beale et al. (2013) observed methanol exchange in both directions in the Atlantic Ocean with a net oceanic emission of 12 Tg yr^{-1}, while Yang et al. (2013) reported a global extrapolation of −42 Tg yr^{-1} based on the atmospheric deposition of methanol over the Atlantic Ocean. In situ methanol production is often observed in oceanic waters (Dixon, Beale, et al., 2013) and phytoplankton could be a key methanol producer (Mincer & Aicher, 2016). However, methanol concentrations are maintained in the nanomolar range due to rapid consumption by marine microorganisms (Beale et al., 2013; Dixon, Beale, et al., 2013; Kameyama et al., 2010; Yang et al., 2013). Microbial uptake of methanol represents a significant biological sink that may reduce oceanic methanol emissions to the atmosphere.

Project Administration: Guang-Chao Zhuang
Resources: Guang-Chao Zhuang, Gui-Peng Yang
Supervision: Guang-Chao Zhuang
Validation: Jiarui Liu, Andrew Montgomery
Visualization: Zhen Zhou
Writing – original draft: Zhen Zhou, Guang-Chao Zhuang
Writing – review & editing: Guang-Chao Zhuang, Jiarui Liu, Zhaohui Chen, Andrew Montgomery, Samantha Joye, Gui-Peng Yang

Methanol can be used as energy source (i.e., methanol being oxidized to CO_2 for energy production) and carbon source (i.e., methanol being assimilated into biomass for cell growth) by methylotrophs or solely used as an energy source by methylovores (Sun et al., 2011). Previous investigations suggested methanol is predominantly oxidized as an energy source in surface ocean; however, it can also be an important source of biomass carbon in high-productivity waters (Dixon, Sargeant, et al., 2013; Zhuang et al., 2018). Methanol concentrations exhibit large spatial and temporal variabilities (ranging from 7 to 429 nM) based on limited observations in the Atlantic and North Pacific waters (Beale et al., 2011, 2013; Kameyama et al., 2010; Yang et al., 2013, 2014). Likewise, a few studies demonstrated that the biological turnover time for methanol varied from 1 to 33 days in marine waters and that rates of methanol metabolism often correlated with environmental variables, such as chlorophyll *a*, nutrients, and heterotrophic bacterial production (BP; Dixon et al., 2011a; Dixon, Sargeant, et al., 2013; Zhuang et al., 2018).

To better understand the sources and sinks of methanol on a global scale, it is critical to delineate methanol distribution and metabolism in a wide range of marine systems. In this study, we report contemporaneous measurements of methanol concentration and consumption rates (i.e., oxidation rates and assimilation rates measured with ^{14}C-labeled methanol) in the northwest Pacific Ocean. Methanol concentrations were determined with a purge and trap preconcentration system, and methanol consumption rates were quantified using radiotracer at environmentally relevant concentrations. Together, these data allowed us to elucidate the role of methanol as a carbon and energy source. This data set expands the global database of methanol concentration, constrains methanol consumption rates in the Pacific Ocean, and provides insights into the biogeochemical cycling of methanol in oceanic waters.

2. Materials and Methods

2.1. Sample Collection and Geochemical Analyses

Samples were collected from the Kuroshio-Oyashio extension (KOE) region in the northwest Pacific Ocean on board R/V "Dongfanghong 3" during an expedition in May 2021 (Figure S1 in Supporting Information S1). KOE is a confluence of the western boundary currents of the subtropical and western subarctic gyres (Xu et al., 2021). Multiscale physical processes in the region impact air-sea exchanges, seawater geochemistry, and marine ecosystems. As such, KOE represents a biological "hotspot" for carbon cycling in the northwest Pacific Ocean (Nagai et al., 2019).

Water samples for geochemical analyses were collected from 18 sites with a Seabird 911 CTD-Niskin rosette system. Nutrient samples (nitrate, nitrite, and phosphate) were passed through a 0.7-μm filter and stored at −20°C before shore-based analyses using Seal Analytical Quaatro nutrient autoanalyzer. Ammonium concentrations were determined by fluorometric method on board immediately after collection without filtration (Holmes et al., 1999; Ning et al., 2013). For chlorophyll *a* analysis, ∼1 L of seawater was filtered through a 0.7-μm Whatman GF/F filter, and the filters were stored at −20°C. Chlorophyll *a* concentrations were measured fluorometrically using an F4500 fluorometer (Hitachi, Japan) (Parsons et al., 1984).

Methanol samples were stored at −80°C before shore-based analyses (Zhuang, Montgomery, et al., 2019). Methanol concentrations were analyzed with a commercial purge and trap system (Acrichi PTC, Beijing Juxin Zhuifeng Technology Co., Ltd). coupled to a gas chromatograph (Agilent GC8890, Agilent Technologies Inc.; modified from Zhuang et al., 2014). Briefly, a 10-mL sample was purged for 10 min at 85°C using ultra-pure nitrogen gas. The evolved gas passed through an absorbent trap (Tenax® TA) and was electrically cooled to −15°C. After sparging, the trap was heated to 200°C and this temperature was held for 4 min. The desorbed methanol was introduced to the gas chromatograph, separated using an HP-PLOT Q capillary column (30 m × 0.32 mm × 20 μm, Agilent), and quantified using a flame ionization detector. A calibration curve was constructed using standards prepared using analytical grade methanol (AR, Sinopharm Chemical Reagent Co., Ltd.) and Milli-Q water. The detection limit of the method was 12 nM and the precision of the method was ∼5%.

2.2. Microbial Assimilation and Oxidation Rate Measurements With ^{14}C-Labeled Methanol

Microbial transformation of methanol, that is, assimilation of methanol into particulate cell biomass (as a carbon source) or oxidation to carbon dioxide (as an energy source), was determined using a radiotracer

19448007, 2023, 8, Downloaded from https://agupubs.onlinelibrary.wiley.com/doi/10.1029/2022GL101605 by Montana State University Library, Wiley Online Library on [07/06/2023]. See the Terms and Conditions (https://onlinelibrary.wiley.com/terms-and-conditions) on Wiley Online Library for rules of use; OA articles are governed by the applicable Creative Commons License

19448007, 2023, 8, Downloaded from https://agupubs.onlinelibrary.wiley.com/doi/10.1029/2022GL101605 by Montana State University Library, Wiley Online Library on [07/06/2023]. See the Terms and Conditions (https://onlinelibrary.wiley.com/terms-and-conditions) on Wiley Online Library for rules of use; OA articles are governed by the applicable Creative Commons License

approach, as described previously by Zhuang et al. (2018). For tracer preparation, a ^{14}C-methanol primary stock (50 mCi mmol^{-1}, American Radiolabeled Chemicals) was diluted with sterile Milli-Q water to generate working solutions. Seawater samples were collected in quadruplicate (a killed control and triplicate live samples) and transferred to 56 mL serum vials that were sealed without a headspace. Before tracer addition, control samples were killed by injecting 2.8 mL 100% trichloroacetic acid (TCA, a final concentration of 5%) through the stopper. After that, 100 μL ^{14}C-methanol (~1,500 Bq) solution was injected into live and control samples through the stopper by replacing 100 μL of seawater. The samples were then incubated in the dark at in situ temperature for 48 hr.

After incubation, a 30-mL subsample was collected with a syringe by displacement with the same volume of N_2; the displaced water was collected into a second syringe and then transferred into a 50-mL centrifuge tube. Microbial activity was terminated immediately by adding ~1.5 mL 100% TCA and this subsample was used to quantify assimilation rates. Another ~1.3 mL of 100% TCA was injected into the remaining 26 mL sample in the serum vial, which was stored for determination of methanol oxidation rates.

For assimilation rates, a 30-mL subsample was filtered onto a 0.22-μm GWSP filter membrane (polyethersulfone, Millipore). The filter was rinsed with 35‰ NaCl solution, placed in a 7-mL scintillation vial and filled with 6 mL scintillation cocktail (Ultima Gold Cocktail, PerkinElmer). Methanol assimilation was measured using a liquid scintillation counter (Tri-Carb®3110TR, PerkinElmer). Methanol oxidation rates were quantified by tracking $^{14}CO_2$ production from added tracer. The 26 mL subsample was acidified by the addition of TCA and purged with N_2. The stripped $^{14}CO_2$ passed through an ice-cold acidic purification trap (1 M phosphoric acid in 15 mL centrifuge tube; minimize the contamination of $^{14}CH_3OH$) and trapped in a mixture of 4.5 mL of scintillation cocktail and 1.5 mL 3-methoxypropylamine (Sigma-Aldrich).

Assimilation or oxidation turnover rate constants (k, day^{-1}) were calculated from Equation 1:

$$k = \frac{f}{t} \tag{1}$$

where f is the ratio of the recovered ^{14}C activity (particulates on the filter or evolved $^{14}CO_2$) divided by added $^{14}CH_3OH$ activity; t is the incubation time (day). The turnover time (day) is the reciprocal of the rate constant. All rate constants were corrected by subtracting killed control counts. Assimilation or oxidation rates were calculated from the turnover rate constant (k) and in situ methanol concentration ($C_{\text{in situ}}$, Equation 2):

$$\text{Rate} = k \times C_{\text{in situ}} \tag{2}$$

Total methanol uptake, representing methanol transport into the cell, was calculated as the sum of the assimilation and the oxidation rates.

2.3. Estimation of Methanol Air-Sea Flux

The air-sea flux was calculated based on a two-layer model from Liss and Slater (1974) (Equation 3):

$$F = K_t\left(\left(\frac{C_a}{H}\right) - C_w\right) \tag{3}$$

where C_w and C_a are the seawater and atmospheric concentrations of methanol, respectively. Atmospheric methanol concentrations were not measured, so we used an average value of 0.57 ppb for the Pacific, as reported previously (Singh et al., 2004). H is the dimensionless Henry's Law constant (corrected for temperature and salinity; Johnson, 2010). K_t is the total gas transfer velocity calculated by Equation 4:

$$\frac{1}{K_t} = \frac{1}{k_w} + \frac{1}{Hk_a} \tag{4}$$

where k_w (water gas transfer velocity) and k_a (air gas transfer velocity) are calculated from Equation 5 (Nightingale et al., 2000) and Equation 6 (Duce et al., 1991), respectively:

$$k_w = \left(0.222 \times u_{10}^2 + 0.333 \times u_{10}\right)\left(\frac{Sc_w}{Sc_{600}}\right)^{-0.5} \tag{5}$$

$$k_a = \frac{u_{10}}{770 + 45 \times \mathrm{MW}^{1/3}} \quad (6)$$

where u_{10} is the wind speed measured at 10 m above the sea surface, MW is the molecular weight of methanol (32.04 g mol^{-1}), Sc_w is the Schmidt number of methanol (corrected by temperature and salinity), and Sc_{600} represents the Schmidt number for CO_2 in fresh water at 20°C (600).

2.4. Bacterial Production

Heterotrophic BP was quantified by tracking ^{3}H-leucine incorporation (Kirchman, 2001); the details of this method were described by Zhuang, Peña-Montenegro, et al. (2019). Bacterial carbon production (BCP) was calculated based on the measured BP rate (i.e., leucine incorporation rate, nmol L^{-1} day^{-1}), the median of empirical leucine conversion factor (LCF) in the open ocean (0.56 kg C/mol leucine; Giering & Evans, 2022), and the molar mass of carbon (MM, 12 g mol^{-1}).

$$\mathrm{BCP} = \frac{\mathrm{BP} \times \mathrm{LCF}}{\mathrm{MM}} \quad (7)$$

Bacterial carbon demand (BCD), including production and respiration, represents the amount of carbon required to support physiological activity. The BCD was estimated from BCP (μg C L^{-1} hr^{-1} in Equation 8) and the bacterial growth efficiency (BGE). BGE was calculated with an experiential model, which described the relationships between BGE and BCP based on previous measurements (Equation 9; del Giorgio & Cole, 1998):

$$\mathrm{BCD} = \frac{\mathrm{BCP}}{\mathrm{BGE}} \quad (8)$$

$$\mathrm{BGE} = \frac{0.037 + 0.65\mathrm{BCP}}{1.8 + \mathrm{BCP}} \quad (9)$$

3. Results and Discussion

3.1. Water Column Biogeochemistry and Distribution of Methanol in the KOE Region

Seawaters were sampled from the KOE region across a number of study sites (Figure S1 in Supporting Information S1). In these areas, hydrographic properties and seawater chemistry were significantly impacted by the Kuroshio current from the south and the Oyashio current from the north (Table 1). Chlorophyll *a* concentrations in the surface waters varied significantly between sites (0.1–2.9 μg L^{-1}). The highest abundance of chlorophyll *a* (2.9 μg L^{-1}) at site D6 in the Oyashio extension, was ∼9 times of the average chlorophyll *a* concentration at other sites (0.3 μg L^{-1}), indicating the occurrence of an algae bloom during sampling. Lower concentrations (<0.2 μg L^{-1}) were found at sites in the Kuroshio extension (e.g., D1, D2, and E9). The average concentrations were slightly higher than the values observed previously in autumn in the KOE (0.02–0.3 μg L^{-1}; Xu et al., 2023). Likewise, nitrate concentrations were much higher at northern sites (e.g., >1.0 μM at E8, E12, and D5, a maximum of 4.0 μM at D6) than those in the south (e.g., <LOD at D1 and D2). Similar patterns were observed for other nutrients (Table 1). Phosphate concentrations ranged from 0.02 μM at D1 to 0.5 μM at E8. Concentrations of nitrite and ammonium were generally lower than 0.2 μM (i.e., D6) and 0.57 μM (i.e., E8), respectively. Nutrient concentrations were comparable to values previously reported for this region (Lin et al., 2020; Wang et al., 2022; Xu et al., 2023).

BP rates exhibited large variability between sites, ranging from 0.8 nmol leucine L^{-1} day^{-1} at E8 to 9.0 nmol leucine L^{-1} day^{-1} at D6, with an average of 5.0 nmol leucine L^{-1} day^{-1}. Methanol was detected at most sites with concentrations ranging from 13 to 391 nM (Table 1). The highest concentrations were observed at stations D1 (339 nM), E9 (391 nM), and E10 (324 nM). These concentrations were generally within the wide range measured previously in marine waters (<27–429 nM; Beale et al., 2011, 2013; Kameyama et al., 2010; Williams et al., 2004; Yang et al., 2013). In the western North Pacific Ocean, methanol concentrations varied between 78 and 325 nM; slightly higher than the concentrations observed in our study area (Kameyama et al., 2010).

Likely sources of methanol in pelagic surface waters include in situ biological and photochemical production (Dixon, Beale, et al., 2013), or to a lesser extent, atmospheric deposition, which depends on sea-air exchange flux.

19448007, 2023, 8, Downloaded from https://agupubs.onlinelibrary.wiley.com/doi/10.1029/2022GL101605 by Montana State University Library, Wiley Online Library on [07/06/2023]. See the Terms and Conditions (https://onlinelibrary.wiley.com/terms-and-conditions) on Wiley Online Library for rules of use; OA articles are governed by the applicable Creative Commons License

19448007, 2023, 8, Downloaded from https://agupubs.onlinelibrary.wiley.com/doi/10.1029/2022GL101605 by Montana State University Library, Wiley Online Library on [07/06/2023]. See the Terms and Conditions (https://onlinelibrary.wiley.com/terms-and-conditions) on Wiley Online Library for rules of use; OA articles are governed by the applicable Creative Commons License

Table 1
Overview of Sampling Sites and Geochemistry of the Surface Water in the KOE Region

Site	Longitude	Latitude	Mixed layer depth[a]	Euphotic depth[b]	Temperature	Methanol	Salinity	NH_4^+	NO_3^-	NO_2^-	PO_4^{3-}	Chlorophyll	Bacterial production
	(E)	(N)	(m)	(m)	(°C)	(nM)		(nM)	(μM)	(μM)	(μM)	(μg L^{-1})	(nmol Leu L^{-1} day^{-1})
D1	145°01.89	30°22.59	15	198	24.1	339	34.6	17	B.D.	B.D.	0.02	0.1	5.0
D2	146°18.87	32°34.36	11	173	21.4	31	34.8	17	B.D.	B.D.	0.03	0.1	6.6
D3	147°37.04	35°00.73	22	N.D.	20.4	19	34.7	B.D.	B.D.	B.D.	0.1	0.1	5.9
D4	148°48.85	37°00.92	12	146	18.4	B.D.	34.3	73	0.1	0.03	0.1	0.5	5.5
D5	149°52.12	38°56.89	40	N.D.	11.2	19	34.6	135	1.6	0.1	0.2	0.8	1.6
D6	151°12.05	40°59.78	26	N.D.	10.4	B.D.	33.6	181	4.0	0.2	0.4	2.9	9.0
E1	146°29.10	33°59.46	26	123	21.2	19	34.7	24	0.03	B.D.	0.04	0.1	N.D.
E2	146°31.24	35°30.17	40	N.D.	19.9	21	34.7	17	B.D.	B.D.	0.03	0.1	4.6
E3	146°30.13	37°00.07	26	171	20.1	B.D.	34.6	24	B.D.	B.D.	0.05	0.1	N.D.
E4	146°29.69	38°31.16	30	N.D.	17.0	60	34.6	140	0.4	0.05	0.1	0.7	1.7
E5	147°59.95	33°58.15	52	107	21.3	77	34.7	15	0.1	B.D.	0.04	0.2	N.D.
E6	147°59.50	37°00.11	21	N.D.	16.8	B.D.	34.4	195	0.1	B.D.	0.1	0.6	6.7
E7	148°00.00	38°30.17	27	N.D.	17.0	13	34.4	93	1.2	0.1	0.2	0.6	6.6
E8	147°59.87	40°00.04	15	79	11.1	B.D.	32.7	574	2.3	0.1	0.5	0.8	0.8
E9	150°50.53	33°59.62	16	118	22.4	391	34.6	14	B.D.	B.D.	0.04	0.1	6.5
E10	149°59.22	35°31.03	15	232	20.9	324	33.3	18	B.D.	B.D.	0.03	0.1	5.5
E11	150°03.06	36°59.96	22	N.D.	21.9	52	34.5	26	0.02	0.03	0.03	0.1	5.4
E12	150°00.29	39°59.83	26	N.D.	22.1	50	34.3	49	1.2	0.1	0.2	0.4	4.2

Note. B.D.: Below the detection limit. N.D.: Not determined.

[a]The depth with a difference of 0.2°C from 10 m temperature was considered as the base of the mixed layer (de Boyer Montégut et al., 2004). [b]The euphotic depth was determined that photosynthetically available radiation (PAR) is 1% of its surface value (Lee et al., 2007).

Dixon, Beale, et al. (2013) measured methanol production rates of 49–103 nmol L^{-1} day^{-1} in the Atlantic Ocean, while photoproduction seemed to play an inconsequential role in gross in situ production. These results are supported by a later study, which demonstrated that methanol can be produced by a broad phylogenetic array of marine phytoplankton (Mincer & Aicher, 2016). However, methanol concentrations did not correlate with chlorophyll concentration in our study area. The ability of phytoplankton to produce methanol was species-dependent (Mincer & Aicher, 2016). For example, *Emiliania huxleyi* released much more methanol (~5.3 ± 1.0 fmol $cell^{-1}$) than *Prochlorococcus* (~0.05 ± 0.01 fmol $cell^{-1}$) in the cultures (Mincer & Aicher, 2016). Therefore, the lack of correlation between methanol and chlorophyll might be attributed to the presence of distinct methanol producers among phytoplankton species in this area. Furthermore, the chlorophyll as a proxy of phytoplankton biomass could be largely affected by the light and nutrient-driven photoacclimation in the northwest Pacific (Xing et al., 2021). Once produced, methanol can be rapidly consumed by microbes. Ultimately, the balance of production and consumption determines the standing concentrations of methanol in marine waters, which could be regulated by complex physical, biological, or photochemical processes.

Depth profiles of methanol and other variables were measured at sites D2 and D6 (Figure S2 in Supporting Information S1). A deep chlorophyll *a* maximum was detected at ~55 m (0.7 μg L^{-1}) at D2 (Figure S2 in Supporting Information S1). Methanol accumulated in the upper 100 m and a maximum of 73 nM was observed at 15 m. Below 125 m, methanol was barely detected in the deep waters with exceptions of 17 and 19 nM at 5,000 and 5,853 m, respectively. In contrast, chlorophyll *a* concentrations peaked at 15 m (3.7 μg L^{-1}) and decreased to 0.03 μg L^{-1} at 75 m at site D6. A peak of methanol concentration (184 nM) was documented at 175 m; concentrations were less than 30 nM at other depths. Methanol accumulation in surface waters or in subsurface maxima was often observed in previous studies (Beale et al., 2013; Williams et al., 2004), which measured methanol concentrations in the upper 200 m waters. The subsurface maxima, also detected in this study, could be related

19448007, 2023, 8, Downloaded from https://agupubs.onlinelibrary.wiley.com/doi/10.1029/2022GL101605 by Montana State University Library, Wiley Online Library on [07/06/2023]. See the Terms and Conditions (https://onlinelibrary.wiley.com/terms-and-conditions) on Wiley Online Library for rules of use; OA articles are governed by the applicable Creative Commons License

Table 2
Microbial Assimilation and Oxidation of Methanol in the KOE Region

Site	Assimilation k (day^{-1})	Oxidation k (day^{-1})	Assimilation rate (nmol L^{-1} day^{-1})	Oxidation rate (nmol L^{-1} day^{-1})	Oxidation/total uptake (%)
D1	0.001 ± 0.0002	0.39 ± 0.02	0.24 ± 0.07	130.5 ± 6.8	99.8
D2	0.013 ± 0.004	0.21 ± 0.02	0.41 ± 0.13	6.5 ± 0.6	94.0
D3	0.005 ± 0.001	0.05 ± 0.01	0.09 ± 0.02	0.9 ± 0.1	90.8
D4[a]	0.017 ± 0.001	0.27 ± 0.01	0.20 ± 0.01	3.3 ± 0.2	94.3
D5	0.011 ± 0.002	0.24 ± 0.01	0.21 ± 0.03	4.5 ± 0.2	95.6
D6[a]	0.013 ± 0.001	0.23 ± 0.09	0.16 ± 0.01	2.7 ± 1.0	94.5
E2	0.014 ± 0.004	0.23 ± 0.01	0.30 ± 0.09	4.8 ± 0.2	94.2
E6[a]	0.012 ± 0.002	0.27 ± 0.09	0.15 ± 0.03	3.3 ± 1.1	95.7
E7	0.012 ± 0.001	0.21 ± 0.01	0.15 ± 0.01	2.7 ± 0.1	94.6
E8[a]	N.D.	0.15 ± 0.07	N.D.	1.7 ± 0.9	N.D.
E9	0.017 ± 0.003	0.18 ± 0.003	6.83 ± 0.98	71.1 ± 1.3	91.2
E12	0.024 ± 0.005	0.21 ± 0.02	1.23 ± 0.26	10.7 ± 0.9	89.7

Note. N.D.: Not determined.
[a]Metabolic rates were calculated using methanol concentrations of 12 nM (i.e., the limit of detection) for those samples below the detection limit.

to elevated production or reduced degradation in this layer. In addition to phytoplankton release, methanol can be produced from the degradation of large biomolecules, such as pectin and lignin (Donnelly & Dagley, 1980; Schink & Zeikus, 1980). Accumulation of exported particles and organic matter in the subsurface might also lead to the elevated level of methanol. However, no consistent trend was observed in depth profiles between sites in this, and in previous studies (Beale et al., 2013), further suggesting the complex control of methanol in the ocean. Additionally, methanol was generally not detected in waters deeper than 200 m. This is not surprising given the dominant source of methanol via phytoplankton production or photochemical process in the photic zone. BP of methanol from organic matter, including pectin and lignin, may provide an alternative source of methanol in deep waters (Donnelly & Dagley, 1980; Schink & Zeikus, 1980).

3.2. Microbial Metabolism of Methanol as a Carbon and Energy Source

The assimilation of added $^{14}CH_3OH$ tracer into biomass and its oxidation to $^{14}CO_2$ were detected in surface waters at 12 sites. Methanol assimilation rate constants varied significantly between 0.001 and 0.024 day^{-1} (average: 0.013 ± 0.006 day^{-1}) (Table 2). Maximum and minimum assimilation rate constants were observed at E12 and D1, respectively. Assimilation rate constants were lower than reported values for coastal waters but fell within the wide range measured in the oligotrophic gyres of the Atlantic Ocean and surface waters in the Gulf of Mexico (Dixon, Sargeant, et al., 2013; Zhuang et al., 2018). Microbial oxidation of $^{14}CH_3OH$ to $^{14}CO_2$ was much faster than assimilation to biomass, with an average oxidation rate constant of 0.22 day^{-1}. The maximum oxidation rate constant at site D1 (0.39 day^{-1}) was about eight times higher than the lowest observed at D3 (0.05 day^{-1}). Oxidation rate constants were among the highest values documented in the oligotrophic tropical North East Atlantic (turnover time: 1–25 days) (Dixon et al., 2011b), and the turnover times were as low as 3 days (3–19 days) in surface waters of KOE region.

By combining measured rate constants with in situ methanol concentrations, we estimated methanol assimilation and oxidation rates. Assimilation rates ranged from 0.09 to 6.8 nmol L^{-1} day^{-1}, and the maximum rate occurred at site E9, where the highest methanol concentration was observed. In contrast, methanol oxidation was highest at site D1, with a rate of 130.5 nmol L^{-1} day^{-1}. The overall rates (1.0–130.7 nmol L^{-1} day^{-1}) were comparable to those high rates (between 2 and 146 nmol L^{-1} day^{-1}) in the tropical Atlantic (Dixon et al., 2011b). The rapid turnover and high methanol oxidation rates could also explain the relatively low methanol concentrations observed in the KOE region.

Linear relationships between methanol assimilation and oxidation, and biogeochemical variables such as chlorophyll *a*, BP, or nutrients were not apparent. Previous studies reported significant linear correlations between

19448007, 2023, 8, Downloaded from https://agupubs.onlinelibrary.wiley.com/doi/10.1029/2022GL101605 by Montana State University Library, Wiley Online Library on [07/06/2023]. See the Terms and Conditions (https://onlinelibrary.wiley.com/terms-and-conditions) on Wiley Online Library for rules of use; OA articles are governed by the applicable Creative Commons License

methanol metabolisms and environmental factors (e.g., chlorophyll *a*, primary production, BP, and nutrients) in the Gulf of Mexico (Zhuang et al., 2018) and Atlantic Ocean (Dixon, Sargeant, et al., 2013). These data sets covered diverse geographical and biogeochemical areas, including both coastal and deep waters. The controls of methanol metabolism are likely more complex in the KOE region since mixing of different water masses generates dynamic physical (e.g., temperature), chemical (e.g., nutrients), and biological (e.g., chlorophyll *a*) conditions, all of which can influence the activity of methanol-utilizing microorganisms.

Methanol oxidation rates were much higher than the assimilation rates, and $^{14}CO_2$ production accounted for 89.7%–99.8% (average: 94.1%) of the total utilization of methanol. Hence, methanol was used predominantly as an energy source and only a minor fraction of methanol was assimilated into biomass. Previous studies also reported that >90% of methanol was respired to CO_2 for energy production in the oligotrophic oceanic waters of the Gulf of Mexico and Atlantic Ocean (Dixon et al., 2011b; Zhuang et al., 2018). In contrast, up to 35% and 57% of methanol was used as a carbon source in the nutrient-rich coastal waters (Dixon et al., 2011b; Zhuang et al., 2018). Similar scenarios were also observed for the metabolism of other low molecular weight carbon compounds, such as acetate and dimethylsulfoniopropionate (DMSP); their role as biomass-carbon sources may be more important in nutrient-rich coastal regions compared to the oligotrophic open ocean (Motard-Côté et al., 2016; Zhuang, Peña-Montenegro, et al., 2019). Presumably, elevated nutrient levels and microbial activity underscore the higher carbon demand to support the biomass growth of heterotrophs in coastal waters. Furthermore, methylotrophs that utilize C1 compounds including methanol for energy and biomass production are usually more abundant in coastal waters (Halsey et al., 2012; Rappe et al., 2000). In contrast, methylovores that only oxidize C1 compounds such as SAR11 bacteria appear to be much more ubiquitous in global ocean (Sun et al., 2011). Recently, Sargeant et al. (2018) demonstrated that SAR11 made significantly larger contribution to methanol oxidation rates in the open ocean (0.3%–59%) than the coastal waters (<0.01%–2.3%). Therefore, observed differences of methanol cycling in coastal or open ocean areas could be driven by the relative abundance of C1-utilizing microorganisms.

3.3. Estimation of the Contribution of Methanol to BCP and BCD

Using the measured leucine incorporation rates, we calculated the BCP rates that ranged from 73 to 419 nmol C L^{-1} day^{-1} in the KOE region (Table S1 in Supporting Information S1). Accordingly, BCD was estimated to be 2.2×10^3–4.9×10^3 nmol C L^{-1} day^{-1} using an experiential model. However, the carbon incorporated from methanol accounted for less than 2.2% of BCP. By comparison, the total uptake of methanol contributed a maximum of 3.3% to the BCD. These values were slightly lower than previous estimations in the North Atlantic (~13%; Dixon et al., 2011b), where methanol likely made a significant contribution to BCD with chlorophyll *a* concentrations <0.2 μg L^{-1}. Nevertheless, methanol contributions to the BCD were comparable to other low molecular weight compounds, such as dissolved DMSP (1.1%–7.0%; Motard-Côté et al., 2016) and acetate (0.1%–4.9%; Zhuang, Peña-Montenegro, et al., 2019), or higher than these for methane (Mao et al., 2022), acrylate (0.01%–0.13%), and dimethylsulfoxide (0.04%–0.14%) (Tyssebotn et al., 2017), suggesting that the role of methanol as a microbial carbon source cannot be neglected for marine microbes. Indeed, C1-utilizing microorganisms are highly diverse and versatile (Halsey et al., 2012; Sargeant et al., 2018; Taubert et al., 2015; Zhuang et al., 2018), and the presence of methanol may provide an alternative substrate for methylotrophs and methylovores in oceanic waters.

3.4. Source or Sink of Oceanic Methanol to the Atmosphere

To assess the oceanic source or sink of methanol to the atmosphere in the KOE region, we used an average atmospheric concentration of methanol in the Pacific measured previously (0.57 ppb; Singh et al., 2004) to calculate the air-sea flux. Air-sea fluxes ranged from −41 to 29 μmol m^{-2} day^{-1} (average: 9 μmol m^{-2} day^{-1}), where a negative value was indicative of emission to the atmosphere (Figure 1). The ocean was a sink of methanol at most sites, except sites D1, E9, and E10, where methanol loss to the atmosphere was estimated. At these sites with negative methanol fluxes, methanol concentrations were relatively high compared to the other study sites. This pattern agrees with previous studies, which reported methanol exchange in both directions in the Atlantic (Beale et al., 2013). The use of an average air-side methanol value of 0.57 ppb will introduce uncertainty into the air-sea flux calculations. However, the calculated atmospheric concentrations of methanol in equilibrium with seawater methanol were either much lower or higher than the adopted value of 0.57 ppb at sites with positive fluxes (0.11 ± 0.09 ppb) or negative fluxes (1.6 ± 0.2 ppb), respectively. Uncertainty might remain for flux estimation, but this uncertainty was unlikely to affect our determinations of whether sites were sinks or sources of methanol.

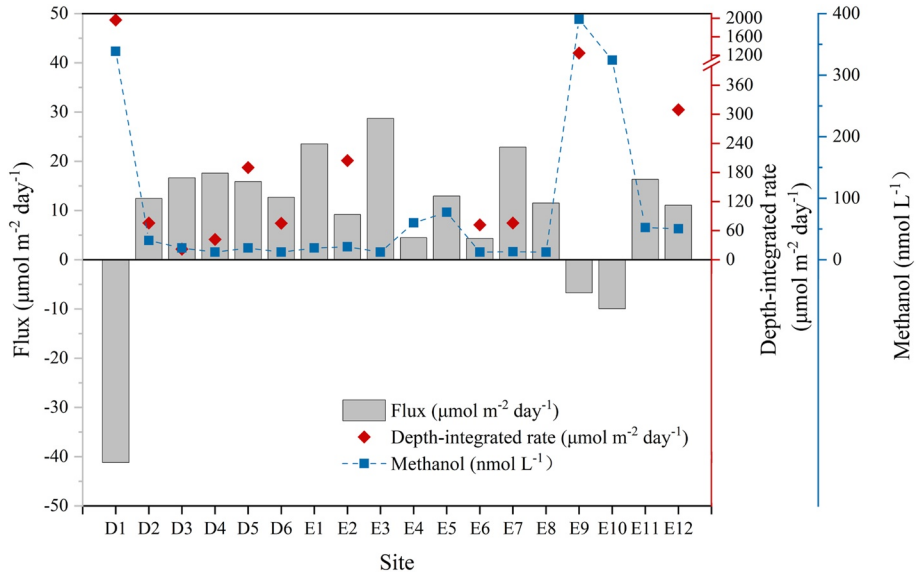

Figure 1. Estimated air-sea exchange flux and depth-integrated consumption rates of methanol in the Kuroshio-Oyashio extension region. Negative values represented methanol emission from the ocean to the atmosphere. Flux was estimated using methanol concentrations of 12 nM (the limit of detection) for sites below the detection limit.

Based on the calculated fluxes, we assessed the relative importance of methanol sources or sinks (e.g., air-sea exchange, in situ production, and microbial consumption). Assuming atmospheric deposition could supply methanol in the mixed layer, we could estimate the balance of methanol source and sink by comparing the depth-integrated consumption rates with air-to-sea flux. By multiplying the mixed layer depth and consumption rates measured at each site, we calculated depth-integrated consumption rates in the mixed layer, which ranged between 22 and 1,961 μmol m^{-2} day^{-1} (Figure 1). The results indicated that atmospheric deposition of methanol to surface waters accounted for 22.7% (3.6%–76.0%; calculated using air-to-sea flux divided by depth-integrated consumption rates at each site) of the total biological consumption of methanol. The gap between atmospheric input and biological loss suggested that significant in situ production supports the mass balance and maintains the methanol pool in the mixed layer. At sites with estimated methanol loss to the atmosphere, ventilation contributed to 0.5% and 2.1% of the total loss (the sum of consumption rates and sea-to-air fluxes) at E9 and D1, respectively. Therefore, microbial consumption was the dominant pathway for methanol removal in the mixed layer of the KOE region. Collectively, the pool sizes of methanol are largely dependent on the differences of production and consumption at specific sites, which determined whether the ocean was a source or sink of methanol relative to the atmosphere.

4. Conclusion

In this study, we investigated methanol concentrations and metabolic rates simultaneously in the KOE region of northwest Pacific Ocean. Methanol concentrations varied significantly between sites (<12–391 nM). The relatively low concentrations could be attributed to rapid biological turnover of methanol, as revealed by the high consumption rates measured. Methanol oxidation accounted for >89.7% of total uptake rates, suggesting that methanol is predominantly used as an energy source. Methanol uptake accounted for a maximum of 3.3% of the BCD, indicating an important role for methanol in microbial carbon metabolism. Based on estimated air-sea exchange fluxes in the study area, the KOE region was considered as a net sink with respect to atmospheric methanol. Air-sea flux accounted for 22.7% of microbial consumption in the mixed layer, suggesting that atmospheric deposition was a minor source of methanol to surface waters and in situ production was more important for maintenance of the methanol pool. These results constrain the in situ concentrations and biological metabolism of methanol in the oceanic waters of northwest Pacific, illustrate the relative importance of different sources/sinks (e.g., atmospheric deposition, in situ production, and microbial consumption), and improve our current understanding of the biogeochemical cycling of methanol in marine systems.

19448007, 2023, 8, Downloaded from https://agupubs.onlinelibrary.wiley.com/doi/10.1029/2022GL101605 by Montana State University Library, Wiley Online Library on [07/06/2023]. See the Terms and Conditions (https://onlinelibrary.wiley.com/terms-and-conditions) on Wiley Online Library for rules of use; OA articles are governed by the applicable Creative Commons License

Data Availability Statement

The data set has been deposited in the PANGAEA database at https://www.pangaea.de (https://doi.org/10.1594/PANGAEA.952087 (Zhou et al., 2023a) and https://doi.org/10.1594/PANGAEA.952265 (Zhou et al., 2023b)).

Acknowledgments
The authors acknowledge the captain, crew, and scientists of the R/V "Dongfanghong 3" for their kind assistance and cooperation during sampling. This work was financially supported by the National Natural Science Foundation of China (Grant 42076031), the Taishan Scholars Program of Shandong Province (Grant tsqn201909057), the National Key Research and Development Program of China (Grant 2022YFE0136300), and the Fundamental Research Funds for the Central Universities (Grants 202072001 and 202041008).

References

Beale, R., Dixon, J. L., Arnold, S. R., Liss, P. S., & Nightingale, P. D. (2013). Methanol, acetaldehyde, and acetone in the surface waters of the Atlantic Ocean. *Journal of Geophysical Research: Oceans*, *118*(10), 5412–5425. https://doi.org/10.1002/jgrc.20322

Beale, R., Liss, P. S., Dixon, J. L., & Nightingale, P. D. (2011). Quantification of oxygenated volatile organic compounds in seawater by membrane inlet-proton transfer reaction/mass spectrometry. *Analytica Chimica Acta*, *706*(1), 128–134. https://doi.org/10.1016/j.aca.2011.08.023

de Boyer Montégut, C., Madec, G., Fischer, A. S., Lazar, A., & Iudicone, D. (2004). Mixed layer depth over the global ocean: An examination of profile data and a profile-based climatology. *Journal of Geophysical Research*, *109*(C12), C12003. https://doi.org/10.1029/2004JC002378

del Giorgio, P. A., & Cole, J. J. (1998). Bacterial growth efficiency in natural aquatic systems. *Annual Review of Ecology and Systematics*, *29*(1), 503–541. https://doi.org/10.1146/annurev.ecolsys.29.1.503

Dixon, J. L., Beale, R., & Nightingale, P. D. (2011a). Microbial methanol uptake in northeast Atlantic waters. *The ISME Journal*, *5*(4), 704–716. https://doi.org/10.1038/ismej.2010.169

Dixon, J. L., Beale, R., & Nightingale, P. D. (2011b). Rapid biological oxidation of methanol in the tropical Atlantic: Significance as a microbial carbon source. *Biogeosciences*, *8*(9), 2707–2716. https://doi.org/10.5194/bg-8-2707-2011

Dixon, J. L., Beale, R., & Nightingale, P. D. (2013). Production of methanol, acetaldehyde, and acetone in the Atlantic Ocean. *Geophysical Research Letters*, *40*(17), 4700–4705. https://doi.org/10.1002/grl.50922

Dixon, J. L., Sargeant, S., Nightingale, P. D., & Colin Murrell, J. (2013). Gradients in microbial methanol uptake: Productive coastal upwelling waters to oligotrophic gyres in the Atlantic Ocean. *The ISME Journal*, *7*(3), 568–580. https://doi.org/10.1038/ismej.2012.130

Donnelly, M. I., & Dagley, S. (1980). Production of methanol from aromatic acids by *Pseudomonas putida*. *Journal of Bacteriology*, *142*(3), 916–924. https://doi.org/10.1128/jb.142.3.916-924.1980

Duce, R. A., Liss, P. S., Merrill, J. T., Atlas, E. L., Buat-Menard, P., Hicks, B. B., et al. (1991). The atmospheric input of trace species to the world ocean. *Global Biogeochemical Cycles*, *5*(3), 193–259. https://doi.org/10.1029/91GB01778

Giering, S. L. C., & Evans, C. (2022). Overestimation of prokaryotic production by leucine incorporation—And how to avoid it. *Limnology & Oceanography*, *67*(3), 726–738. https://doi.org/10.1002/lno.12032

Halsey, K. H., Carter, A. E., & Giovannoni, S. J. (2012). Synergistic metabolism of a broad range of C1 compounds in the marine methylotrophic bacterium HTCC2181. *Environmental Microbiology*, *14*(3), 630–640. https://doi.org/10.1111/j.1462-2920.2011.02605.x

Heikes, B. G., Chang, W., Pilson, M. E. Q., Swift, E., Singh, H. B., Guenther, A., et al. (2002). Atmospheric methanol budget and ocean implication. *Global Biogeochemical Cycles*, *16*(4), 8081–8013. https://doi.org/10.1029/2002GB001895

Holmes, R. M., Aminot, A., Kérouel, R., Hooker, B. A., & Peterson, B. J. (1999). A simple and precise method for measuring ammonium in marine and freshwater ecosystems. *Canadian Journal of Fisheries and Aquatic Sciences*, *56*(10), 1801–1808. https://doi.org/10.1139/f99-128

Johnson, M. T. (2010). A numerical scheme to calculate temperature and salinity dependent air-water transfer velocities for any gas. *Ocean Science*, *6*(4), 913–932. https://doi.org/10.5194/os-6-913-2010

Kameyama, S., Tanimoto, H., Inomata, S., Tsunogai, U., Ooki, A., Takeda, S., et al. (2010). High-resolution measurement of multiple volatile organic compounds dissolved in seawater using equilibrator inlet–proton transfer reaction-mass spectrometry (EI–PTR-MS). *Marine Chemistry*, *122*(1), 59–73. https://doi.org/10.1016/j.marchem.2010.08.003

Kirchman, D. (2001). Measuring bacterial biomass production and growth rates from leucine incorporation in natural aquatic environments. *Methods in Microbiology*, *30*, 227–237. https://doi.org/10.1016/S0580-9517(01)30047-8

Lee, Z., Weidemann, A., Kindle, J., Arnone, R., Carder, K. L., & Davis, C. (2007). Euphotic zone depth: Its derivation and implication to ocean-color remote sensing. *Journal of Geophysical Research: Oceans*, *112*(C3), C03009. https://doi.org/10.1029/2006JC003802

Lin, G., Chen, Y., Huang, J., Wang, Y., Ye, Y., & Yang, Q. (2020). Regional disparities of phytoplankton in relation to different water masses in the Northwest Pacific Ocean during the spring and summer of 2017. *Acta Oceanologica Sinica*, *39*(5), 107–118. https://doi.org/10.1007/s13131-019-1511-6

Liss, P. S., & Slater, P. G. (1974). Flux of gases across the air-sea interface. *Nature*, *247*(5438), 181–184. https://doi.org/10.1038/247181a0

Mao, S.-H., Zhang, H.-H., Zhuang, G.-C., Li, X.-J., Liu, Q., Zhou, Z., et al. (2022). Aerobic oxidation of methane significantly reduces global diffusive methane emissions from shallow marine waters. *Nature Communications*, *13*(1), 7309. https://doi.org/10.1038/s41467-022-35082-y

Mincer, T. J., & Aicher, A. C. (2016). Methanol production by a broad phylogenetic array of marine phytoplankton. *PLoS One*, *11*(3), e0150820. https://doi.org/10.1371/journal.pone.0150820

Motard-Côté, J., Kieber, D. J., Rellinger, A., & Kiene, R. P. (2016). Influence of the Mississippi River plume and non-bioavailable DMSP on dissolved DMSP turnover in the northern Gulf of Mexico. *Environmental Chemistry*, *13*(2), 280–292. https://doi.org/10.1071/EN15053

Nagai, T., Otsuka, K., & Nakano, H. (2019). The research advancements and historical episodes brought by the Kuroshio flowing across generations. *Kuroshio Current*, 13–22. https://doi.org/10.1002/9781119428428.ch2

Nightingale, P. D., Malin, G., Law, C. S., Watson, A. J., Liss, P. S., Liddicoat, M. I., et al. (2000). In situ evaluation of air-sea gas exchange parameterizations using novel conservative and volatile tracers. *Global Biogeochemical Cycles*, *14*(1), 373–387. https://doi.org/10.1029/1999GB900091

Ning, Z., Liu, S., & Ren, J. (2013). A contrast on various determination methods of ammonium. *Marine Environmental Science*, *32*(5), 763–766.

Parsons, T. R., Maita, Y., & Lalli, C. M. (1984). 4.1 – Determination of chlorophylls and total carotenoids: Spectrophotometric method. In *A manual of chemical & biological methods for seawater analysis* (pp. 101–104). Pergamon.

Rappé, M. S., Vergin, K., & Giovannoni, S. J. (2000). Phylogenetic comparisons of a coastal bacterioplankton community with its counterparts in open ocean and freshwater systems. *FEMS Microbiology Ecology*, *33*(3), 219–232. https://doi.org/10.1111/j.1574-6941.2000.tb00744

Sargeant, S. L., Murrell, J. C., Nightingale, P. D., & Dixon, J. L. (2018). Basin-scale variability of microbial methanol uptake in the Atlantic Ocean. *Biogeosciences*, *15*(16), 5155–5167. https://doi.org/10.5194/bg-15-5155-2018

Schink, B., & Zeikus, J. G. (1980). Microbial methanol formation: A major end product of pectin metabolism. *Current Microbiology*, *4*(6), 387–389. https://doi.org/10.1007/BF02605383

Singh, H. B., Chen, Y., Staudt, A., Jacob, D., Blake, D., Heikes, B., & Snow, J. (2001). Evidence from the Pacific troposphere for large global sources of oxygenated organic compounds. *Nature*, *410*(6832), 1078–1081. https://doi.org/10.1038/35074067

19448007, 2023, 8, Downloaded from https://agupubs.onlinelibrary.wiley.com/doi/10.1029/2022GL101605 by Montana State University Library, Wiley Online Library on [07/06/2023]. See the Terms and Conditions (https://onlinelibrary.wiley.com/terms-and-conditions) on Wiley Online Library for rules of use; OA articles are governed by the applicable Creative Commons License

Singh, H. B., Salas, L. J., Chatfield, R. B., Czech, E., Fried, A., Walega, J., et al. (2004). Analysis of the atmospheric distribution, sources, and sinks of oxygenated volatile organic chemicals based on measurements over the Pacific during TRACE-P. *Journal of Geophysical Research: Atmosphere*, *1099*(D15), D15S07. https://doi.org/10.1029/2003JD003883

Sun, J., Steindler, L., Thrash, J. C., Halsey, K. H., Smith, D. P., Carter, A. E., et al. (2011). One carbon metabolism in SAR11 pelagic marine bacteria. *PLoS One*, *6*(8), e23973. https://doi.org/10.1371/journal.pone.0023973

Taubert, M., Grob, C., Howat, A. M., Burns, O. J., Dixon, J. L., Chen, Y., & Murrell, J. C. (2015). XoxF encoding an alternative methanol dehydrogenase is widespread in coastal marine environments. *Environmental Microbiology*, *17*(10), 3937–3948. https://doi.org/10.1111/1462-2920.12896

Tyssebotn, I. M. B., Kinsey, J. D., Kieber, D. J., Kiene, R. P., Rellinger, A. N., & Motard-Côté, J. (2017). Concentrations, biological uptake, and respiration of dissolved acrylate and dimethylsulfoxide in the northern Gulf of Mexico. *Limnology & Oceanography*, *62*(3), 1198–1218. https://doi.org/10.1002/lno.10495

Wang, Y., He, X., Huang, J., Lin, Y., & Kang, J. (2022). The population of *Trichodesmium* cyanobacteria in the northern Pacific Ocean associated with Kuroshio Extension. *Aquatic Sciences*, *84*(3), 44. https://doi.org/10.1007/s00027-022-00873-4

Williams, J., Holzinger, R., Gros, V., Xu, X., Atlas, E., & Wallace, D. W. R. (2004). Measurements of organic species in air and seawater from the tropical Atlantic. *Geophysical Research Letters*, *31*(23), L23S06. https://doi.org/10.1029/2004GL020012

Xing, X., Boss, E., Chen, S., & Chai, F. (2021). Seasonal and daily-scale photoacclimation modulating the phytoplankton chlorophyll-carbon coupling relationship in the mid-latitude Northwest Pacific. *Journal of Geophysical Research: Oceans*, *126*(10), e2021JC017717. https://doi.org/10.1029/2021JC017717

Xu, F., Yan, S.-B., Zhang, H.-H., Wu, Y.-C., Ma, Q.-Y., Song, Y.-C., et al. (2021). Occurrence and cycle of dimethyl sulfide in the western Pacific Ocean. *Limnology & Oceanography*, *66*(7), 2868–2884. https://doi.org/10.1002/lno.11797

Xu, F., Zhang, H.-H., Yan, S.-B., Sun, M.-X., Wu, J.-W., & Yang, G.-P. (2023). Biogeochemical controls on climatically active gases and atmospheric sulfate aerosols in the western Pacific. *Environmental Research*, *220*, 115211. https://doi.org/10.1016/j.envres.2023.115211

Yang, M., Beale, R., Liss, P., Johnson, M., Blomquist, B., & Nightingale, P. (2014). Air–sea fluxes of oxygenated volatile organic compounds across the Atlantic Ocean. *Atmospheric Chemistry and Physics*, *14*(14), 7499–7517. https://doi.org/10.5194/acp-14-7499-2014

Yang, M., Nightingale, P. D., Beale, R., Liss, P. S., Blomquist, B., & Fairall, C. (2013). Atmospheric deposition of methanol over the Atlantic Ocean. *Proceedings of the National Academy of Sciences of the United States of America*, *110*(50), 20034–20039. https://doi.org/10.1073/pnas.1317840110

Zhou, Z., Zhuang, G.-C., Mao, S.-H., Liu, J., Li, X.-J., Liu, Q., et al. (2023a). Methanol distribution and metabolic rate in the northwest Pacific Ocean in May/June 2021 [Dataset]. PANGAEA. https://doi.org/10.1594/PANGAEA.952087

Zhou, Z., Zhuang, G.-C., Mao, S.-H., Liu, J., Li, X.-J., Liu, Q., et al. (2023b). Depth profile of methanol in site D2 and site D6 in the northwest Pacific Ocean in May 2021 [Dataset]. PANGAEA. https://doi.org/10.1594/PANGAEA.952265

Zhuang, G.-C., Lin, Y.-S., Elvert, M., Heuer, V. B., & Hinrichs, K.-U. (2014). Gas chromatographic analysis of methanol and ethanol in marine sediment pore waters: Validation and implementation of three pretreatment techniques. *Marine Chemistry*, *160*(20), 82–90. https://doi.org/10.1016/j.marchem.2014.01.011

Zhuang, G.-C., Montgomery, A., Samarkin, V. A., Song, M., Liu, J., Schubotz, F., et al. (2019). Generation and utilization of volatile fatty acids and alcohols in hydrothermally altered sediments in the Guaymas Basin, Gulf of California. *Geophysical Research Letters*, *46*(5), 2637–2646. https://doi.org/10.1029/2018GL081284

Zhuang, G.-C., Peña-Montenegro, T. D., Montgomery, A., Hunter, K. S., & Joye, S. B. (2018). Microbial metabolism of methanol and methylamine in the Gulf of Mexico: Insight into marine carbon and nitrogen cycling. *Environmental Microbiology*, *20*(12), 4543–4554. https://doi.org/10.1111/1462-2920.14406

Zhuang, G.-C., Peña-Montenegro, T. D., Montgomery, A., Montoya, J. P., & Joye, S. B. (2019). Significance of acetate as a microbial carbon and energy source in the water column of Gulf of Mexico: Implications for marine carbon cycling. *Global Biogeochemical Cycles*, *33*(2), 223–235. https://doi.org/10.1029/2018GB006129

19448007, 2023, 8, Downloaded from https://agupubs.onlinelibrary.wiley.com/doi/10.1029/2022GL101605 by Montana State University Library, Wiley Online Library on [07/06/2023]. See the Terms and Conditions (https://onlinelibrary.wiley.com/terms-and-conditions) on Wiley Online Library for rules of use; OA articles are governed by the applicable Creative Commons License